WFPC2 Synphot Update

S. Baggett, S. Casertano, S. Gonzaga, C. Ritchie
October 13, 1997

ABSTRACT

The STSDAS tables used by synphot to provide the photometric calibration information in the image headers have been updated on the basis of new calibration data. All UV filters shortward of F439W were updated, as well as some of the more frequently-used broad-band filters redward of F439W (F450W, F555W, F606W, F675W, F702W, F785LP, F791W, F814W, F850LP, and F1042M). Changes were installed in the OPUS pipeline on May 16, 1997. With a few exceptions, changes to non-UV filter modes were relatively minor: generally ~1-2% or less (changes in F785LP, F850LP, and F1042M were higher: ~1-4%, ~1-6%, and ~2-15% respectively, depending on the chip.). The UV filters required somewhat larger changes to bring synphot into agreement with the observations, ranging from ~2% (e.g., F255W and F300W) to ~5% (F170W, F218W) to 10% or more (F160BW, F375N). Any filters not updated at this time will be checked with observations recently executed and updated later in 1997 if necessary.

1. Introduction

The synphot package in STSDAS has three primary uses: 1) to provide photometric calibration information, which is inserted by the calibration software into image headers (keywords PHOTFLAM, PHOTBW, etc); 2) to use synthetic photometry to calibrate observations; and 3) to estimate exposure times for HST observations. The focus of this ISR will be on the photometric calibration and population of the header keywords.

The pipeline calibration software (**calwp2)** uses the wfpc2-related **synphot** tables to populate the photometric keywords in the calibrated header (c0h), without changing any of the data values. These keywords, listed in Table 1, identify the properties of the filter(s) used and define the absolute photometric calibration of the observations. Specifically, the keywords PHOTMODE, PHOTPLAM, and PHOTBW give the observing mode, pivot wavelength and bandwidth of the filter/detector combination used. PHOTFLAM gives the conversion factor from measured count rates in the image to the corresponding source flux, for an assumed flat spectrum (constant flux per unit wavelength). Note that all these keywords, except for the table names (see below), are group keywords, as they can be different from chip to chip. Group keywords can be accessed through STSDAS tasks such as **hedit** and **imhead**.

Table 1: Photometric Header Keywords

keyword	description	example	name used by STSDAS
PHOTMODE	observation mode	WFPC2,1,A2D7,F300W,,CAL	OBSMODE
PHOTFLAM	inverse sensitivity[a]	5.926793E-17 erg/sec/cm^2/Å	URESP
PHOTZPT	zeropoint	-21.1mag	PHOTZPT
PHOTPLAM	pivot wavelength	2990.016 Å	PIVWV
PHOTBW	RMS bandwidth of the filter	324.5099 Å	BANDW
GRAPHTAB	HST graph table used in pipeline	h5l1440cm.tmg	same
COMPTAB	HST component table	h5g10115m.tmc	same

a.PHOTFLAM is the flux conversion factor, the flux that produces 1 count/sec in the passband. See the STSDAS Synphot User's Guide for more details on the definitions of these keywords.

The table names given in the calibrated header (c0h) keywords GRAPHTAB and COMPTAB are generic keywords; the names themselves encode the time of installation of the table[1]. Since these tables (GRAPHTAB and COMPTAB) are used by all instruments, it is likely that new tables are installed in the pipeline between WFPC2 table deliveries; these tables will have different names, but they will contain exactly identical information as far as WFPC2 observations are concerned. The HST graph table (.tmg) is used to determine all of the necessary components for each observing mode, such as the HST OTA, WFPC2 optics, filter, chip response, etc. The HST component table determines which version of each individual component table (e.g., hst_ota_005.tab, wfpc2_optics_004.tab) is used in the calculation of the photometric keywords. In Appendix B, we provide an example of tracing an observation mode path through the HST graph and component tables. Note, however, that normally, you will not need to trace the paths manually, as the files used for computing the photometric values are listed in the calibrated headers (c0h) and/or can be determined by running the STSDAS **showfiles** command.

The version of the tables used in the calibration of a science images can be determined by either checking the GRAPHTAB and COMPTAB names or looking at the header HISTORY records. For the update described here (May 1997), the table names provided by the GRAPH and COMPTAB keywords should start with h5 or later (h6, h7, etc). Alternatively, the calibrated header files (c0h) produced by the pipeline contain HISTORY

1. For example, the COMPTAB table name mentioned above (h5g10115m.tmc) can be decoded as: h=year since 1980 (=1997), 5 is month (May), g is the day (16th), etc.

keywords which provide a detailed list of the WFPC2 **synphot** table versions used to populate the photometric keywords. For example, the **synphot**-related HISTORY keywords in the header of an older PC1, F300W observation were:

```
HISTORY The following throughput tables were used:crotacomp$hst_ota_005.tab,
HISTORY crwfpc2comp$wfpc2_optics_003.tab,crwfpc2comp$wfpc2_f300w_003.tab,
HISTORY crwfpc2comp$wfpc2_dqepc1_002.tab,crwfpc2comp$wfpc2_a2d7pc1_002.tab,
HISTORY crwfpc2comp$wfpc2_flatpc1_001.tab
```

The STSDAS **showfiles** task provides a listing of the tables for any specified observation mode and can be used to check if new tables are available:

```
> showfiles wfpc2,1,a2d7,f300w,cal
#Throughput table names:
crotacomp$hst_ota_005.tab
crwfpc2comp$wfpc2_optics_004.tab
crwfpc2comp$wfpc2_f300w_004.tab
crwfpc2comp$wfpc2_dqepc1_003.tab
crwfpc2comp$wfpc2_a2d7pc1_002.tab
crwfpc2comp$wfpc2_flatpc1_001.tab
```

Since the local **synphot** table directories at STScI are kept up-to-date[2], the **showfiles** output reflects the most current set of tables; in the example above, the optics, filter, and DQE tables have been updated since the PC1, F300W observation was processed.

2. History of Previous Synphot Table Changes

The **synphot** tables for WFPC2 have been updated about once a year since the original 1994 pre-launch version, which was based on predicted throughput and ground test results. Not all of the updates, however, affect all observations modes; we provide below a short description of the changes affecting WFPC2.

1995

The first update was installed in the pipeline on July 20, 1995. The new tables were computed on the basis of inflight observations of the spectrophotometric standard GRW+70D5824 (DA3 white dwarf with V=12.77 and B-V = -0.09), the star on which most of our photometric calibration is based. With this update, the WFPC2 **synphot** results were brought into general agreement with the IDT results (Holtzman et al. 1995a; 1995b); see also WFPC2 Instrument Handbook, Version 3.0, June 1995)); *this update affected most observation modes*. As per **synphot** definition, the tables provided flux predictions appropriate for an aperture with radius 3”, assuming an aperture correction of 0.10 magnitudes between aperture radii of 0.5’’ (used for the WFPC2 calibration photometry measurements) and 3’’. A 4%/800 pixel linear ramp correction for the CTE problem was applied to the measurements in order to derive the flux calibration, which is therefore applicable to observations at x=0 (in practice, ~2% was added to the measurements, since

2. For information on retrieving and updating your local table versions, please refer to the online Guide to the WFPC2 Synphot Tables, on the WFPC2 Documentation page.

the target was well-centered in each chip[3]). Before this update, the **synphot** tables contained pre-launch throughput estimates based on ground test data. Typical changes were ~5-10%, although some modes were a bit higher (~15-20%); a few observation modes were not updated at this time because of the lack of data (e.g., methane quads, ramp filters, and a few of the less commonly used UV filters).

1996

Two WFPC2 **synphot** table updates were installed in 1996, affecting only a small number of observing modes. An update of only the linear ramp filter (LRF) table was performed on Feb 8, 1996; prior to this, the table was merely a placeholder. The updated table (wfpc2_lrf_002.tab) provides a preliminary photometric calibration accuracy of ~3% for the ramp filter modes. The LRF setting should be included in the observation mode via the keyword 'lrf#nnnn', where the nnnn represents the central wavelength for the observation (e.g., "wfpc2,2,lrf#5007,a2d7"[4]); note that the pipeline does not yet automatically include the LRF term. More details about the generation and use of this table are described in WFPC2 ISR #96-06, "The Photometric Calibration of WFPC2 Linear Ramp Filter Data in Synphot."

The second update was installed on June 27. This update, based again on observations of our standard star GRW+70D5824, was implemented to bring the predicted throughput for the methane and UV [OII] quad filters into better agreement with those observations. This update affected the filter curves for the 6193 Å and 8929 Å methane quad filters (apertures FQCH4N33, FQCH4N15, FQCH4P15, and FQCH4W3) and the UV quad filters (apertures WF2, WF3, WF4, and FQUVN33). The adjustments consisted of scaling the filter throughputs down (by 3-15% for all except FQCH4P15, which was scaled down by 30%) and fixing an incorrect path (FQUVN33) in the graph table. The throughputs for the unrotated methane quad used with WF2 or WF4 (mean wavelengths 5433 and 7274, respectively) were not changed.

3. The Current Update

The main motivation for a new update to the **synphot** tables is the availability of a more complete set of observations for the UV throughput. While **synphot** could be relied upon to predict the throughput in most visible and red filters to within 2-5%, the lack of sufficient UV data had prevented us from obtaining a comparable accuracy for the UV filters. A specific program of UV throughput observations was carried out in Cycles 5 and 6, using all UV filters, before and after a decontamination, in each of the four chips. Some

---

3. A straight 4% linear ramp was used for this update. Note however, that recent results suggest the CTE loss depends on X and Y positions, on the background counts, and on the star brightness (see ISR 97-08, "New Results on Charge Transfer Efficiency and Constraints on Flat-Field Accuracy.").
4. The double quotes are mandatory around any obsmode containing the '#' character.

observations with crossed filters were also included to obtain more detailed information on the wavelength dependence of the detectors' sensitivity in the far UV.

In addition to the new UV observations, we also took advantage of the photometric observations accumulated over three years via our bimonthly photometric monitor, which consists of throughput measurements for the ‘‘standard’’ filter set (F160BW, F218W, F255W, F336W, F439W, F555W, F675W, and F814W. The throughput numbers are as given in TIR 97-01). Observations were taken in PC1 and WF3 during Cycles 4 and 5, and through a different chip each month for Cycle 6. Generally, we have between 10 and 25 observations for each observing mode, except for F170W (~60, observations are done in all 4 chips each month) and F555W (~60 in PC1, observations taken every month).

This update to the WFPC2 **synphot** tables consists primarily of a new determination of the detector quantum efficiency (DQE) for all four chips. For the first time, different curves were determined for each chip. In addition, the overall efficiencies of the UV filters were rescaled, in a few cases (F343N and F375N) by significant amounts. Because the DQE curves were changed, *ALL observation modes are affected*. The changes are generally small (< 2%) for visible and red filters, while changes of 10% or more are seen for many UV filters.

As a test of the **synphot** table update, we compared predictions based on the new **synphot** tables to measurements obtained for the same UV spectrophotometric standard star, GRW+70D5824, from the photometric zeropoint calibration program. These included PC1 and WF3 images in all medium and wide broadband filters longwards of F380W that were not covered by the photometric monitoring program. The comparisons will be extended in the future using other stars, both blue and red, for which some data have recently been obtained.

The Method: general discussion

The overall throughput of WFPC2 consists of five terms: the OTA transmission, the WFPC2 optics, the detector quantum efficiency (DQE), the filter transmission, the aperture correction, and the gain[5]. In this update we kept the gain fixed at its nominal value; note that all observations were taken using the Bay 3 electronics (with nominal gain 14 e/count). Holtzman et al. (1995b) give the appropriate conversion factors for Bay 4 electronics (gain 7). The OTA transmission was multiplied by 0.9108 to correct for the internal obscuration of WFPC2, and the aperture correction was *defined* to be 0.1 mag between an aperture of 0.5’’ radius (the standard aperture for photometry) and 3” radius. These two terms very nearly cancel, and had been mistakenly omitted in the previous **synphot** tables; the net effect of their inclusion is less than 1%.

5. There is also a flatfield table built into the WFPC2 observing mode paths (see examples in Section 1), but the table is just a placeholder and has no effect on the results; the flatfield term is not used because it is not necessary.

Aperture Corrections

A note of caution is necessary on the subject of aperture corrections. By definition, **synphot** predicts *total* counts (in DN if the a2d term is included in the obsmode, in electrons if it is omitted), and thus refers nominally to an infinite aperture. However, the use of very large apertures is impractical in most cases, and can introduce very large uncertainties because of the large number of pixels involved. We recommend that all point source photometry be referred to the standardized aperture of 0.5'' radius suggested in Holtzman et al. (1995b). Measured aperture corrections between 0.5'' and 3'' radius are generally around 0.1 mag (see Holtzman 1995a), but they fluctuate from filter to filter and have significant uncertainties (probably about 0.02 mag). In order to maintain the nominal definition of **synphot** without introducing the uncertainties associated with aperture corrections to large radii, we define the total counts at "nominal infinity" as $10^{(0.10/2.5)}$ multiplied by the counts within 0.5'' radius; this is equivalent to defining the aperture correction for 0.5'' to nominal infinity as 0.1 magnitudes, irrespective of filter. This should not affect the absolute calibration of point sources for the majority of applications. However, the calibration of extended sources should use the actual aperture correction to infinity, which can be determined from the Holtzman (1995a) tables, instead of the nominal 0.1 mag adopted here, and correct the **synphot** predictions appropriately.

DQE and Filter Curve Updates

The bulk of the corrections applied here involve the filter transmissions and the DQE curves. For the filters, the *shape* of the transmission curves is kept fixed, allowing only for an overall scaling factor for each curve. For the DQE curves we considered only smooth changes as a function of wavelength, represented by low-order polynomials, but we did allow each detector's curve to be changed independently. Of course, filter transmission and DQE are to some extent complementary; in general, it is impossible to completely disentangle the contribution of the filter and of the DQE, since only their product is directly observable (except for the few cases with crossed filters). Our goal was to achieve a good match between predictions and observations while minimizing the changes required. The differences between cameras in the same filter were attributed to different DQE between the detectors, since the filter curves are the same for all detectors. On the other hand, if the predictions for an individual filter deviated from the observations consistently in the four chips, then rescaling the filter curve was considered more appropriate. Note that, since the wavelength coverages of many filters overlap, changes in the DQE curves tend to affect the predicted response in several filters, and thus the changes in DQE and filter curves must be made simultaneously and consistently.

The Method: explicit algorithm

The procedure we followed consists of four steps. First, we added the WFPC2 obscuration term and the aperture correction in the **synphot** tables since previous versions of **synphot** only included the obscuration due to the OTA secondary mirror. In order to account for the obscuration in the Cassegrain repeater inside the WFPC2, we multiplied the wfpc2_optics table, used by **synphot**, by the factor 0.9108. For the aperture term, we assumed a constant correction of 0.10 mag between the 0.5'' radius aperture and infinity, and thus multiplied the DQE curve, determined by Holtzman et al. (1995) for the 0.5'' aperture, by the factor $1.0965=10^{(0.10/2.5)}$, independent of wavelength. For example, in the case of PC1, the corrections were implemented as

wfpc2_optics_new(throughput) = wfpc2_optics_003.tab(throughput)[6] * 0.9108

wfpc2_dqepc1_new(throughput) = wfpc2_dqepc1_002.tab(throughput) * (10**(0.1/2.5)

Similar equations determine the DQE for the WF chips. These two corrections combined made a change of less than 0.2% in the total throughput estimate. Once these changes were applied, the resulting set of **synphot** tables were used to generate count rate predictions, which were ratioed to the observed count rate adjusted for a CTE correction (~0.02 magnitudes) and an aperture correction (0.10 magnitudes at all wavelengths).

Second, we determined an average smooth correction to the DQE curve for the four chips. For each filter, we used the average response of all four chips and compared that to the response predicted by **synphot** (as described in the first step). We then determined the DQE that produced the best fit to the observed counts, using the weighted least-squares method described below. The DQE change was described by a fourth-order polynomial, which seemed adequate to remove the systematic deviations between predicted and observed counts as a function of wavelength.

Third, we rescaled individual filters to exactly match the average counts in all four chips. We used only an overall scale factor, without any modifications to the shape of each filter curve. This step brought the average predicted and observed counts into exact agreement. Generally, the necessary renormalizations were quite small, ~1-2%. Exceptions to this were F343N (~50%), F375N (~15%), and F185W (~20%); these three filters had not been adjusted since before launch. For example, F170W required a 1.014 scale factor:

wfpc2_f170w_new(throughput) = wfpc2_f170w_003(throughput) * 1.014

Fourth, we introduced another smooth correction to the DQE, also in the form of a fourth-order polynomial, but this time different for each chip, in order to account for the chip-to-chip differences for each filter. This resulted in the final DQE curves and predicted

---

6. Note: in practice, we performed the operations on copies of the previous **synphot** table versions (version 3 of the optics table and version 2 of the DQE tables); the table numbers are incremented after installation in the pipeline (e.g., wfpc2_optics_new is now wfpc2_optics_004).

counts for each chip, and in most cases reduced the differences between predictions and observations in individual chips.

In principle, we could have obtained similar final results by skipping Step 2 and applying individual rescalings directly to each filter in Step 3, thus obtaining the same exact agreement between average predicted and observed counts as the procedure outlined above. However, we chose to follow the above procedure, applying the smooth DQE change before the filter scalings, for two reasons. First, obvious trends in the predicted vs. observed counts (see Figure 1 below) are more likely to be due to a smooth variation of the DQE rather than to individual filters being coherently offset as a function of wavelength. If this interpretation is correct, changing the DQE before filter scalings is more likely to produce good results for spectral shapes different from our standard star. Second, applying filter scalings first could introduce sharp variations of the predicted vs. observed counts as a function of wavelength, which would then be hard to correct in individual detectors.

Figure 1: Trends in predicted versus observed throughput ratio, using previous version of **synphot** tables (1995/6).

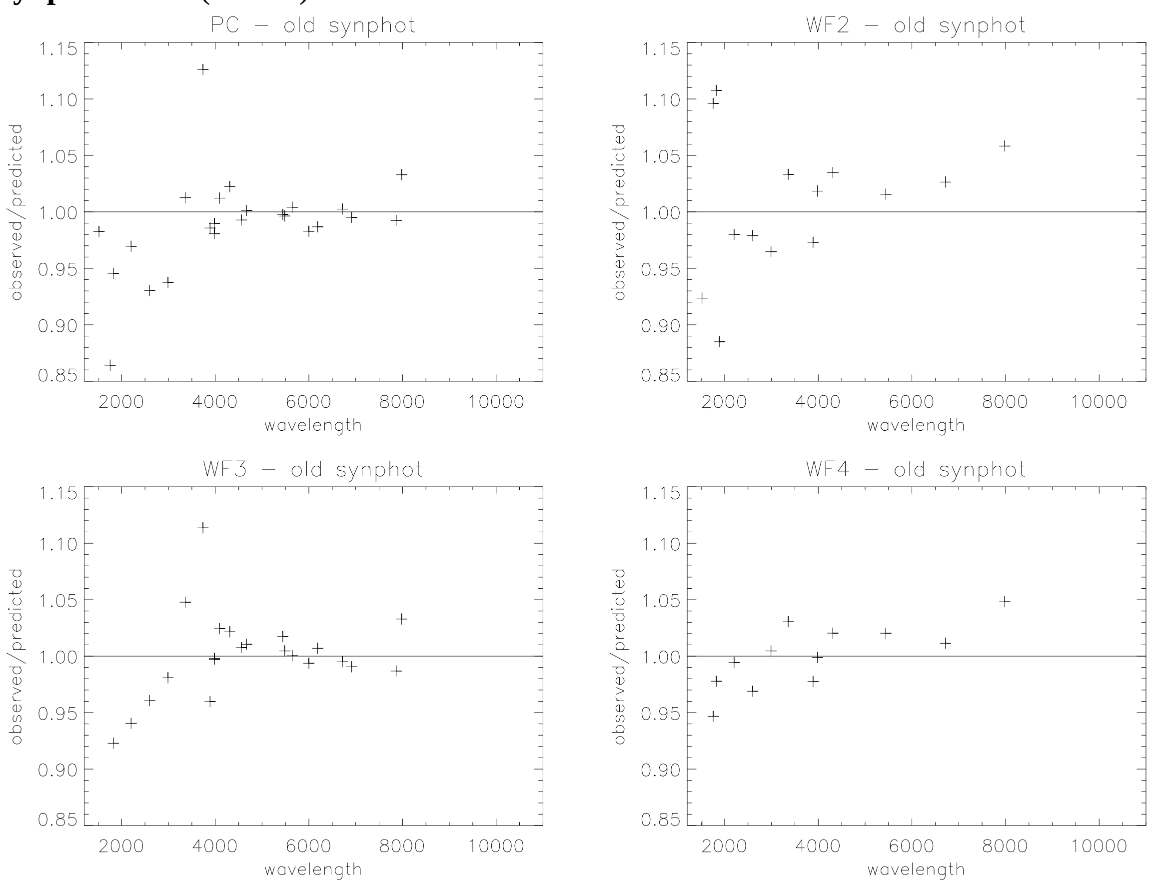

Least-squares adjustment for the DQE

A major component of the current **synphot** update involved adjusting the DQE curves. This was necessary in order to allow for differences between the chips; any changes to the other tables (e.g., filter) affects all chips. We chose this method in order to be able to adjust the DQE tables as a smooth function of wavelength and make full use of the entire bandpass of all available observing modes to determine the solution (rather than adjusting the DQE at just the pivot points of the filters, which would result in an unrealistic final DQE solution).

The essence of the method is to derive the necessary updates by computing and minimizing the χ^2 based on the **synphot** count rate predictions and the corrected count rates over all the UV and photometric monitoring data. The objective of course is to have the **synphot** tables defined in such a way that the observed flux in any given observing mode equals the product of all the relevant throughput tables summed over wavelength, that is,

$$Flux_{filter} = \sum_{\lambda} T(\lambda)_{filter} \cdot DQE(\lambda)$$

Here, the DQE term is only the DQE table and the T term includes all the other **synphot** tables (optics, ota, filter, etc.). We expanded the DQE term, as described in the previous section, into an average smooth DQE term multiplied by a fourth order polynomial which was allowed to vary from chip to chip, that is:

$$DQE = \left(A_0 + A_1\frac{\lambda}{5000.} + A_2\left(\frac{\lambda}{5000}\right)^2 + A_3\left(\frac{\lambda}{5000}\right)^3 + A_4\left(\frac{\lambda}{5000}\right)^4\right) \cdot DQE_{ave}$$

where λ is in Angstroms. The total flux can then be written as an expansion of these terms, our goal being to ultimately solve for the coefficients A_i for each chip:

$$Flux_{filter} = A_0 \cdot F_0 + A_1 \cdot F_1 + A_2 \cdot F_2 + A_3 \cdot F_3 + A_4 \cdot F_4$$

We start with the χ^2, which can then be written as

$$\chi^2 = \sum_{f = filters}\left(\frac{R_f - \sum_j A_j \cdot F_{f,j}}{\sigma_f}\right)^2$$

where R_f is the observed countrate in filter f, σ_f the associated error, and the summation over j the predicted **synphot** countrate. The objective is to minimize the the χ^2 or:

$$-\frac{1}{2}\frac{\partial\chi^2}{\partial A_i} = \sum_{f = filters}\left(\frac{R_f - \sum_j A_j \cdot F_{f,j}}{\sigma_f^2}\right) \cdot F_{f,i} = 0$$

To accomplish this practically, we first rewrote the sums

$$\sum_f \frac{R_f \cdot F_{i,f}}{\sigma_f^2} = \sum_f \sum_j \frac{A_j \cdot F_{f,j} \cdot F_{i,f}}{\sigma_f^2}$$

where i=0,1,2,3,4 and then expanded them; this provided us with a straightforward matrix to solve for the coefficients A_0, A_1, A_2, A_3, and A_4:

$$\sum_{f = filters} R_f \cdot F_{i,f} = A_0 \cdot \left(\sum_{filters} \frac{F_{0,f} \cdot F_{i,f}}{\sigma_f^2} \right) + A_1 \cdot \left(\sum_{filters} \frac{F_{1,f} \cdot F_{i,f}}{\sigma_f^2} \right) + A_2 \cdot \left(\sum_{filters} \frac{F_{2,f} \cdot F_{i,f}}{\sigma_f^2} \right) + etc$$

By solving this set of equations simultaneously, we minimized the discrepancies between the predicted and corrected observed count rates and obtained the necessary corrections to each of the chip DQEs. Figure 2 provides a comparison of the old and new DQE curves.

Figure 2: The DQE curves alone, old (crosses) and new (line).

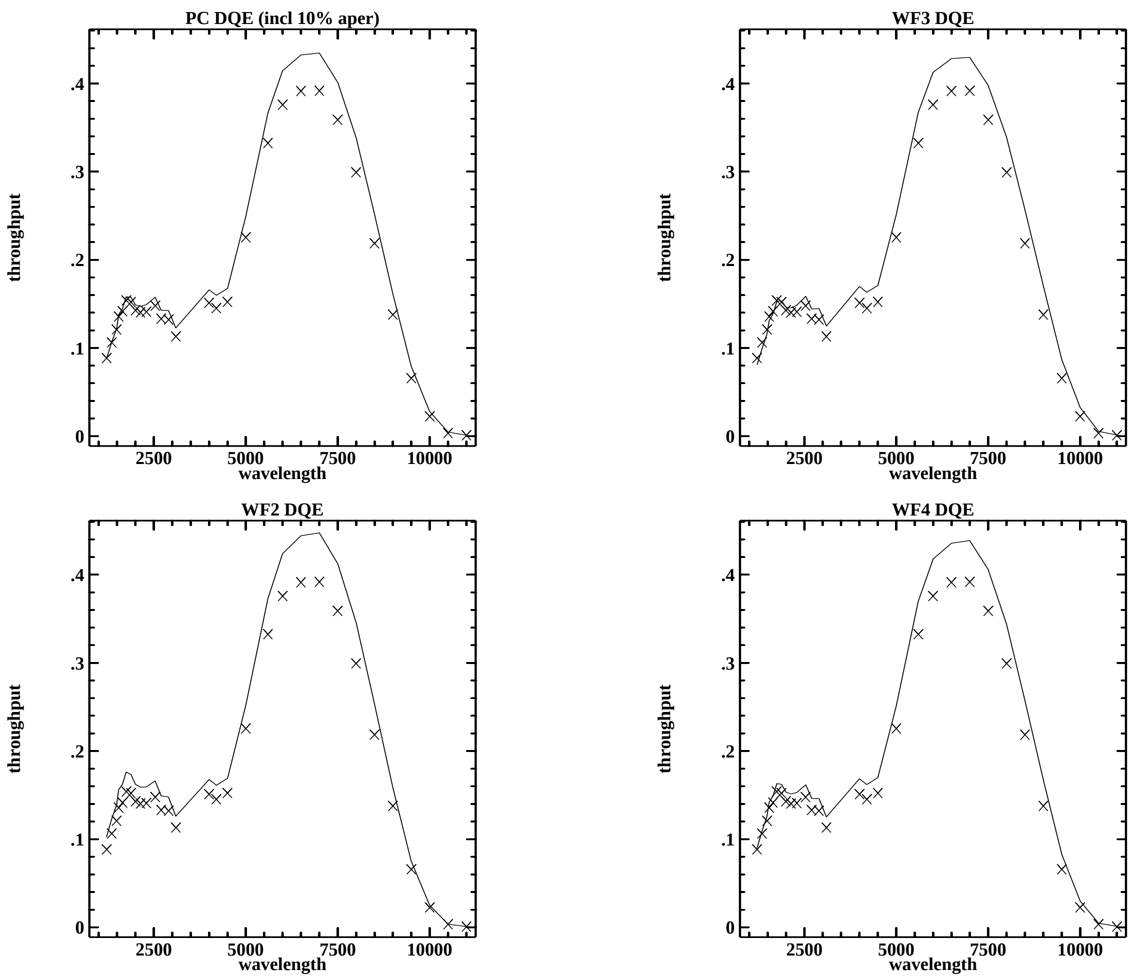

Once the changes were determined using the UV throughput data plus the monitoring data, the **synphot** tables were used to predict countrates for the broadband nonstandard filters to compare to the zeropoint measurements in PC1 and WF3. The resulting throughput ratios (observed countrates corrected for CTE + 10% compared to new **synphot** predicted countrates) are presented in Figure 3 for all data.

Figure 3: Observed throughput compared to updated **synphot** predictions

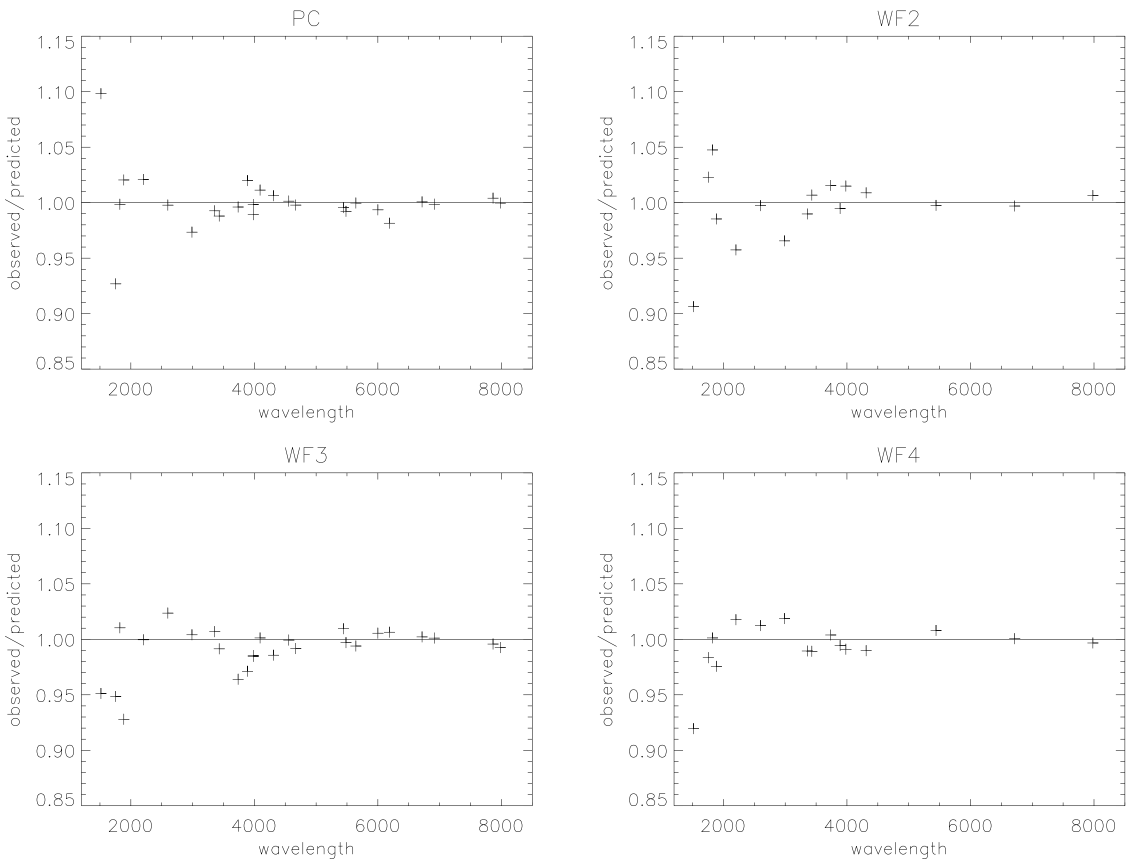

For the most part, the scatter is less than 5%, even in the UV, which is an improvement over the past version of **synphot**, where the scatter was closer to 10%. There are a few minor comments to make about the results.

- There is still more scatter in the UV than in the visible, in all chips. This could not be minimized any further with the available data due to the overlapping filter bandpasses .

- The standard spectrum of GRW+70D5824[7], which only extends to 9202 Angstroms (the limit of the Oke data (Bohlin, 1996)), was adjusted to allow a more reasonable estimation of the most redward observing modes. To avoid having **synphot** zero out the throughput contributions beyond this point, we continued the spectrum out to 30,000 Angstroms; the extrapolation was estimated by scaling a similar white dwarf spectrum (hz43_mod, from Bohlin et al.,1995) to the GRW+70D5824 throughput at F791W.
- In PC1 and WF3, the F1042M data (and to some extent, F850LP) don't fit well (by ~10% and 2% respectively). As described earlier, these two non-standard observing modes were not used to restrict the fits, only the standard filter F814W (photometric monitoring in all 4 chips) was used. Since these two filters are used in less than 2% of external observations, the **synphot** update was installed as-is and the situation for these two filters will be improved once the additional zeropoint calibration is obtained.

4. Updating Image Data with new Synphot Information

If the most recent **synphot** tables were not used during image calibration (see Introduction) the photometric recalibration can be done by, 1) retrieving the PHOTFLAM or zeropoints from the table at the end of this ISR, 2) rerunning **calwp2** after manually updating the appropriate keywords (DOPHOTOM, GRAPHTAB, COMPTAB), or 3) using **synphot** directly (bandpar task). Options 2 and 3 require that the new tables be installed at your site, the tables are available via ftp[8]; the Data Handbook provides more information on rerunning **calwp2**. Appendix A in this report provides a short example of determining PHOTFLAM by running **synphot** directly.

The new PHOTFLAMs and zeropoints for gain 7 are provided in Table 2, in Appendix A. Note that the methane and UV [OII] values are approporiate for gain 15. For other gain 15 observing modes, the gain ratios can be used to adjust the PHOTFLAM in Table 2 (multiply by 1.987, 2.003, 2.006, or 1.955 for PC1, WF2, WF3, and WF4 respectively) or the zeropoint (add -0.745, -0.754, -0.756, or -0.728 for PC1, WF2, WF3, and WF4 respectively). Zeropoints are given in the Vega system; the required conversion factor for transforming ST magnitudes[9] to Vega magnitudes is provided in the 'conv' column. The magnitude of the **synphot** changes are given for PC1 and WF3 in the new/old columns.

---

7. Available via anonymous ftp, in directory /cdbs/cdbs2/calspec/grw_70d5824_005.tab.
8. Ftp ftp.stsci.edu, login as anonymous. Set retrievals for binary format, cd /cdbs/comp/wfpc2, and get wfpc2tar (tarfile contains all wfpc2-related **synphot** tables as well as tables from ota).
9. ST magnitudes are defined as $-2.5*\log_{10}(\mathrm{PHOTFLAM})-21.1$ and result in constant magnitudes for spectra having constant flux per unit wavelength. See STSDAS **Synphot** User's Guide for more details.

5. Summary

The tables used to provide the WFPC2 photometric calibration have been updated and installed in the OPUS pipeline May 16, 1997. Based on data taken with all UV filters plus some of the more popular broadband filters, the changes were made to the WFPC2 optics, filter, and chip-dependent DQE tables. Most changes to the UV observing modes were on the order of 5-10%, while the non-UV changes were ~1-2%. Any filters not updated at this time will be checked with new observations and updated if necessary. In addition, further observations of the white dwarf standard as well as other solar analog standards (P041C, P330E, HZ-44, P177D, S121E, SA 95-330) will be used to verify the new tables and adjust them if necessary.

6. References

Biretta, J., Baggett, S., and Noll, K,. "Photometric Calibration of WFPC2 Linear Ramp Filter Data in Synphot," 1996, *WFPC2 Instrument Science Report* 96-06.

Bohlin, R., "Spectrophotometric Standards from the Far-UV to the Near-IR on the White Dwarf Flux Scale," *AJ* 111, 1743, 1996.

Bohlin, R., Colina, L., and Finley, D., "White Dwarf Standard Stars: G191-B2B, GD 71, GD 153, HZ 43," *AJ* 110, 1316, 1995.

Holtzman, J., Hester, J., Casertano, S., Trauger, J., Ballester, G., Burrows, C., Clarke, J., Crisp, D., Gallegher, J., Griffiths, R., Hoessel, J., Mould, J., Scowen, P., Stapelfeldt, K., Watson, A., and Westphal, J., "The Performance and Calibration of the WFPC2", *PASP* **107**,156, 1995a.

Holtzman, J., Burrows, C., Casertano, S., Hester, J., Trauger, J., Watson, A., Worthey, G., "The Photometric Performance and Calibration of WFPC2" *PASP*, **107**, 1065, 1995b.

"HST Data Handbook," Version 2.0, edited by C. Leitherer, December 1995. (also available via WFPC2 Documentation page http://www.stsci.edu/ftp/instrument_news/WFPC2/wfpc2_doc.html)

Simon, Bernie, "STSDAS Synphot User's Guide," August 1997. (also online at http://ra.stsci.edu/STSDAS.html under Documentation)

Whitmore, B., and Heyer, I., "New Results on Charge Transfer Efficiency and Constraints on Flat-Field Accuracy," *Instrument Science Report* WFPC2 97-08, Sept. 1997.

Whitmore, B., Gonzaga, S., Heyer, I., "Results of the WFPC-2 SMOV Relative Photometry Check," *Technical Instrument Report* WFPC2 97-01 (internal document), April 1997.

WWW Documentation

STSDAS Synphot User's Guide -- *http://ra.stsci.edu/Document.html*

HST Data Handbook -- *http://www.stsci.edu/ftp/documents/html/data-handbook.html*

STSDAS software, documentation, user support -- *http://ra.stsci.edu/STSDAS.html*

WFPC2 Documentation page -- *http://marvel.stsci.edu/ftp/instrument_news/WFPC2/wfpc2_doc.html*

WFPC2 homepage-- *http://www.stsci.edu/ftp/instrument_news/WFPC2/wfpc2_top.html*

All the above sites are also accessible via STSCI's homepage -- *http://www.stsci.edu/*

Any of the online documents may also be requested as paper copies from help@stsci.edu (410-338-1082).

7. Appendix A

The new PHOTFLAMs and zeropoints for gain=7 are listed below (gain=15 for the methane and UV [OII] filters). For other gain=15 observing modes, the gain ratios can be used to adjust the PHOTFLAM or the zeropoint. Zeropoints are given in the Vega system; the required conversion factor used for transforming ST magnitudes[10] to Vega magnitudes is provided in the 'conv' column. Finally, the size of the **synphot** changes are given for PC1 and WF3 in the new/old columns.

Table 2: New PHOTFLAMs and Zeropoints for Gain=7 (Gain=15 for Quad Filters)

filter	PC1				WF2		WF3			WF4	
	new/ old	new PHOT FLAM	conv	Vega ZP	new PHOT FLAM	Vega ZP	new/ old	new PHOT FLAM	Vega ZP	new PHOT FLAM	Vega ZP
f122m	1.021	8.088e-15	-0.363	13.768	7.381e-15	13.868	1.046	8.204e-15	13.752	8.003e-15	13.778
f160bw	1.113	5.212e-15	0.378	14.985	4.563e-15	15.126	1.168	5.418e-15	14.946	5.133e-15	15.002
f170w	1.044	1.551e-15	0.412	16.335	1.398e-15	16.454	1.072	1.578e-15	16.313	1.531e-15	16.350
f185w	1.074	2.063e-15	0.411	16.025	1.872e-15	16.132	1.095	2.083e-15	16.014	2.036e-15	16.040
f218w	1.051	1.071e-15	0.232	16.557	9.887e-16	16.646	1.058	1.069e-15	16.558	1.059e-15	16.570
f255w	1.071	5.736e-16	0.015	17.019	5.414e-16	17.082	1.063	5.640e-16	17.037	5.681e-16	17.029
f300w	1.035	6.137e-17	-0.024	19.406	5.891e-17	19.451	1.019	5.985e-17	19.433	6.097e-17	19.413
f336w	0.980	5.613e-17	-0.098	19.429	5.445e-17	19.462	0.961	5.451e-17	19.460	5.590e-17	19.433
f343n	2.133	8.285e-15	-0.114	13.990	8.052e-15	14.021	2.090	8.040e-15	14.023	8.255e-15	13.994
f375n	0.884	2.860e-15	-0.055	15.204	2.796e-15	15.229	0.865	2.772e-15	15.238	2.855e-15	15.206
f380w	1.008	2.558e-17	0.559	20.939	2.508e-17	20.959	0.987	2.481e-17	20.972	2.558e-17	20.938
f390n	1.035	6.764e-16	0.678	17.503	6.630e-16	17.524	1.012	6.553e-16	17.537	6.759e-16	17.504
f410m	0.999	1.031e-16	0.768	19.635	1.013e-16	19.654	0.977	9.990e-17	19.669	1.031e-16	19.634
f437n	0.997	7.400e-16	0.539	17.266	7.276e-16	17.284	0.978	7.188e-16	17.297	7.416e-16	17.263
f439w	0.984	2.945e-17	0.657	20.884	2.895e-17	20.903	0.965	2.860e-17	20.916	2.951e-17	20.882
f450w	1.008	9.022e-18	0.475	21.987	8.856e-18	22.007	0.992	8.797e-18	22.016	9.053e-18	21.984
f467m	0.997	5.763e-17	0.486	19.985	5.660e-17	20.004	0.981	5.621e-17	20.012	5.786e-17	19.980
f469n	0.996	5.340e-16	0.466	17.547	5.244e-16	17.566	0.982	5.211e-16	17.573	5.362e-16	17.542
f487n	0.996	3.945e-16	-0.054	17.356	3.871e-16	17.377	0.984	3.858e-16	17.380	3.964e-16	17.351
f502n	0.996	3.005e-16	0.260	17.965	2.947e-16	17.987	0.985	2.944e-16	17.988	3.022e-16	17.959

10. ST magnitudes are defined as $-2.5*\log_{10}$(PHOTFLAM)-21.1 and result in constant magnitudes for spectra having constant flux per unit wavelength. See STSDAS Synphot User's Guide for more details.

Table 2: New PHOTFLAMs and Zeropoints for Gain=7 (Gain=15 for Quad Filters)

filter	PC1				WF2		WF3			WF4	
	new/ old	new PHOT FLAM	conv	Vega ZP	new PHOT FLAM	Vega ZP	new/ old	new PHOT FLAM	Vega ZP	new PHOT FLAM	Vega ZP
f547m	0.996	7.691e-18	-0.023	21.662	7.502e-18	21.689	0.993	7.595e-18	21.676	7.747e-18	21.654
f555w	0.998	3.483e-18	-0.000	22.545	3.396e-18	22.571	0.995	3.439e-18	22.561	3.507e-18	22.538
f569w	0.995	4.150e-18	-0.114	22.241	4.040e-18	22.269	0.995	4.108e-18	22.253	4.181e-18	22.233
f588n	0.996	6.125e-17	-0.260	19.172	5.949e-17	19.204	0.998	6.083e-17	19.179	6.175e-17	19.163
f606w	1.010	1.900e-18	-0.316	22.887	1.842e-18	22.919	1.013	1.888e-18	22.896	1.914e-18	22.880
f622w	0.994	2.789e-18	-0.424	22.363	2.700e-18	22.397	1.000	2.778e-18	22.368	2.811e-18	22.354
f631n	0.994	9.148e-17	-0.483	18.514	8.848e-17	18.550	1.002	9.129e-17	18.516	9.223e-17	18.505
f656n	0.993	1.461e-16	-0.924	17.564	1.410e-16	17.603	1.003	1.461e-16	17.564	1.473e-16	17.556
f658n	0.993	1.036e-16	-0.747	18.115	9.992e-17	18.154	1.003	1.036e-16	18.115	1.044e-16	18.107
f673n	0.992	5.999e-17	-0.702	18.753	5.785e-17	18.793	1.002	6.003e-17	18.753	6.043e-17	18.745
f675w	0.998	2.899e-18	-0.703	22.042	2.797e-18	22.080	1.007	2.898e-18	22.042	2.919e-18	22.034
f702w	1.001	1.872e-18	-0.791	22.428	1.809e-18	22.466	1.008	1.867e-18	22.431	1.883e-18	22.422
f785lp	0.988	4.727e-18	-1.525	20.688	4.737e-18	20.692	0.948	4.492e-18	20.738	4.666e-18	20.701
f791w	1.009	2.960e-18	-1.224	21.498	2.883e-18	21.529	1.003	2.913e-18	21.512	2.956e-18	21.498
f814w	1.002	2.508e-18	-1.263	21.639	2.458e-18	21.665	0.988	2.449e-18	21.659	2.498e-18	21.641
f850lp	0.992	8.357e-18	-1.651	19.943	8.533e-18	19.924	0.932	7.771e-18	20.018	8.194e-18	19.964
f953n	0.907	2.333e-16	-1.904	16.076	2.448e-16	16.024	0.827	2.107e-16	16.186	2.268e-16	16.107
f1042m	1.015	1.985e-16	-2.007	16.148	2.228e-16	16.024	0.868	1.683e-16	16.326	1.897e-16	16.197
Gain 15											
fquvn	0.966	1.344e-15	0.240	16.319	8.251e-16	17.369	0.955	1.084e-15	17.042	1.403e-15	16.624
fquvn33	-	-	-	-	1.325e-15	16.334	-	-	-	-	-
fqch4n	-	-	-	-	2.719e-16	17.812	0.883	3.366e-16	16.076	1.651e-16	17.387
fqch4n15	0.955	1.800e-16	-0.433	17.829	-	-	-	-	-	-	-
fqch4p15	0.924	3.518e-16	-1.506	16.028	-	-	-	-	-	-	-
fqch4n33	-	-	-	-	1.758e-16	17.855	-	-	-	-	-

8. Appendix B - Obtaining PHOTFLAMs directly via Synphot

Determine the observation mode of the image using the IRAF **hedit** task:

```
> hedit *101t.c0h[3] photmode .
```

u2ou0101t.c0h[3],PHOTMODE = WFPC2,3,A2D7,F300W,,CAL

Run **synphot** bandpar task, supplying it with the full observation mode

```
> bandpar wfpc2,3,a2d7,f300w,cal output=”” photlist=all
wavetab=””
```

```
# OBSMODE        URESP       PIVWV     BANDW
wfpc2,3,a2d7,f300w,cal  5.9849E-17  2994.3  325.52
# OBSMODE        FWHM        TPEAK     AVGWV
wfpc2,3,a2d7,f300w,cal  766.54  0.0028287  3015.2
# OBSMODE        QTLAM       EQUVW     RECTW
wfpc2,3,a2d7,f300w,cal  8.1829E-4  2.4333  860.23
# OBSMODE        EMFLX       REFWAVE   TLAMBDA
wfpc2,3,a2d7,f300w,cal  5.9004E-14  3015.2  0.0024682
```

Note: if narrowband filters were used, a custom wavetab should be generated using the genwave task since the default wavelength stepsize is sometimes not small enough; e.g.,

```
> genwave wave.tab min=500. max=11000. dwave=1.
> bandpar wfpc2,1,a2d7,f656n,cal output=”” photlist=all
wavetab=wave.tab
```

```
# OBSMODE        URESP       PIVWV     BANDW
wfpc2,1,a2d7,f656n,cal  1.4612E-16  6563.8  53.864
# OBSMODE        FWHM        TPEAK     AVGWV
wfpc2,1,a2d7,f656n,cal  126.84  0.016154  6563.8
# OBSMODE        QTLAM       EQUVW     RECTW
wfpc2,1,a2d7,f656n,cal  6.9749E-5  0.45782  28.341
# OBSMODE        EMFLX       REFWAVE   TLAMBDA
wfpc2,1,a2d7,f656n,cal  4.1783E-15  6563.8  0.016011
```

A ~2.5% difference in the PHOTFLAM value results if the default wavelength table is used for this particular narrowband filter:

```
> bandpar wfpc2,1,a2d7,f656n,cal output=”” photlist=all
wavetab=””
```

```
# OBSMODE        URESP       PIVWV     BANDW
wfpc2,1,a2d7,f656n,cal  1.4256E-16  6564.4  53.154
# OBSMODE        FWHM        TPEAK     AVGWV
wfpc2,1,a2d7,f656n,cal  125.17  0.015698  6564.5
# OBSMODE        QTLAM       EQUVW     RECTW
wfpc2,1,a2d7,f656n,cal  7.1482E-5  0.46923  29.891
# OBSMODE        EMFLX       REFWAVE   TLAMBDA
wfpc2,1,a2d7,f656n,cal  4.2901E-15  6564.5  0.015592
```

9. Appendix C - Tracing an observation mode through the HST graph and component tables.

In this example, we trace a path through the graph (tmg) and HST component table (tmc) to determine which individual throughput files will be used during any **synphot** computations. Assuming an observation mode of “WFPC2,1,A2D7,F336W,,CAL”, we begin by reading the graph table, using the tread task since it is in binary STSDAS format:

```
tread mtab$h5l1440cm.tmg
```

A small portion of the table is shown in Table 3. Paths for all observation modes (all instruments and configurations) are traced starting at INNODE=1; the OUTNODEs point to the next INNODE in the path. We start by searching the keyword column, at INNODE=1, for a keyword from our observation mode. In row 4, we find ‘wfpc2’ with an OUTNODE=20 and note that the component name is ‘clear’. The OUTNODE points us to the next INNODE, that is 20, where we find no keyword from our observation mode, so the ‘default’ keyword (row=8 in Table 2) is used. We take note of the component name, ‘hst_ota’ (the first real component so far, as the previous one was merely ‘clear’) and continue on to INNODE=30. There, we find the ‘wfpc2’ keyword with OUTMODE=7000 (component clear); at INNODE=7000, there is only 1 keyword, default; the component name is wfpc2_optics. We continue to trace the path via the IN-and OUTNODEs, down to F336W, at INNODE=7102, and note the component name (wfpc2_f336w). Then, the path moves through all the remaining filter wheels (in our case, via the ‘default’ keywords) to the last filters at 7110. After that, the path can be traced down to the last OUTNODE for WFPC2 (=7701), for which there is no subsequent INNODE. Such a tracing reveals that the following components will be used by **synphot** for an observation mode of “WFPC2,1,A2D7,F336W,,CAL”:

```
hst_ota
wfpc2_optics
wfpc2_f336w
wfpc2_dqepc1
wfpc2_a2d7pc1
and wfpc2_flatpc1
```

Table 3. Piece of h5l1440cm.tmg (rows have been removed for brevity). Path for the observation mode “WFPC2,1,A2D7,F336W,,CAL” is indicated in bold lettering and marked with arrows for the first few steps.

COMPNAME	KEYWORD	INNODE	OUTNODE
clear	foc	1	20
clear	fos	1	20
clear	wfpc	1	20
clear	**wfpc2**	**1**	**20**
clear	nicmos	1	20
clear	default	1	100
...	...	...	...
hst_ota	**default**	**20**	**30**
hst_ota	ota	20	30
clear	noota	20	30
clear	fos	30	1000
clear	foc	30	2000
...	...	...	...
clear	**wfpc2**	**30**	**7000**
clear	stis	30	8000
clear	nicmos	30	9000
clear	default	100	102
clear	johnson	100	105
clear	cousins	100	200
...	...	...	...
wfpc2_optics	**default**	**7000**	**7100**
wfpc2_f953n	f953n	7100	7101
clear	**default**	**7100**	**7101**
wfpc2_f122m	f122m	7100	7101
wfpc2_f157w	f157w	7100	7101
wfpc2_f160bw	f160bw	7100	7101
clear	**default**	**7101**	**7102**
wfpc2_f130lp	f130lp	7101	7102
wfpc2_f165lp	f165lp	7101	7102
wfpc2_f850lp	f850lp	7101	7102

COMPNAME	KEYWORD	INNODE	OUTNODE
wfpc2_f785lp	f785lp	7101	7102
wfpc2_f336w	**f336w**	**7102**	**7103**
clear	default	7102	7103
wfpc2_f547m	f547m	7102	7103
...	...	...	...
clear	**default**	**7110**	**7200**
...	...	...	...
clear	**1**	**7200**	**7300**
clear	2	7200	7400
clear	3	7200	7500
clear	default	7200	7600
clear	4	7200	7600
clear	**default**	**7300**	**7310**
...	...	...	...
clear	**default**	**7310**	**7320**
wfpc2_lrf	lrf#	7310	7320
wfpc2_dqepc1	**default**	**7320**	**7330**
clear	default	7330	7340
wfpc2_a2d15pc1	a2d15	7330	7340
wfpc2_a2d7pc1	**a2d7**	**7330**	**7340**
clear	**default**	**7340**	**7350**
clear	default	7350	7360
wfpc2_flatpc1	**cal**	**7350**	**7360**
clear	**default**	**7360**	**7700**
wfpc2_contpc1	cont#	7360	7700
...	...	...	...
wfpc2_a2d15wf2	a2d15	7430	7440
wfpc2_a2d7wf2	a2d7	7430	7440
...	...	...	...
clear	**default**	**7700**	**7701**
...	...	...	...

Once the components have been selected, the **synphot** software uses the HST component table (tmc) to find the appropriate versions of the tables to use. This table, as for the graph table, is in binary STSDAS format; using tread, we can examine the contents:

```
tread h5g10115m.tmc
```

A piece of the tmc table has been extracted and is given in Table 4 below, illustrating the individual components for the observation mode in this example. The date and time refer to installation of the files, compname is the name of the individual component, and filename refers to the specific table and version (including directory location logical; please see online WWW Guide to WFPC2 Synphot Tables for more details) which **synphot** will use. As can be seen from the date, July 1995 was the last time the a-to-d files were updated, while most of the other wfpc2 files were changed in this year's update.

Table 4. Some selected rows from the HST component table.

DATE	TIME	COMPNAME	FILENAME
feb 28 1995	4:22:02:000pm	hst_ota	crotacomp$hst_ota_005.tab
jul 20 1995	11:02:22:000sm	wfpc2_a2d7pc1	crwfpc2comp$wfpc2_a2d7pc1_002.tab
jul 20 1995	11:02:22:000am	wfpc2_a2d7wf2	crwfpc2comp$wfpc2_a2d7wf2_002.tab
jul 20 1995	11:02:22:000am	wfpc2_a2d7wf3	crwfpc2comp$wfpc2_a2d7wf3_002.tab
jul 20 1995	11:02:22:000am	wfpc2_a2d7wf4	crwfpc2comp$wfpc2_a2d7wf4_002.tab
may 12 1997	6:55:53:833pm	wfpc2_dqepc1	crwfpc2comp$wfpc2_dqepc1_003.tab
may 12 1997	6:55:53:833pm	wfpc2_dqewfc2	crwfpc2comp$wfpc2_dqewfc2_003.tab
may 12 1997	6:55:53:833pm	wfpc2_dqewfc3	crwfpc2comp$wfpc2_dqewfc3_003.tab
may 12 1997	6:55:53:833pm	wfpc2_dqewfc4	crwfpc2comp$wfpc2_dqewfc4_003.tab
may 12 1997	6:55:53:833pm	wfpc2_f336w	crwfpc2comp$wfpc2_f336w_005.tab
may 12 1997	6:55:53:833pm	wfpc2_optics	crwfpc2comp$wfpc2_optics_004.tab